Mechanisms of Working Memory Impairment in Schizophrenia

Supplemental Information

Supplemental Methods……..p 2 – 7

Table S1…….. p 8 – 9

Table S2…….. p 10 – 11

Table S3…….. p 12 – 13

Table S4…….. p 14

Table S5…….. p 15

Table S6…….. p 16

Table S7…….. p 17 – 18

Table S8…….. p 19 – 21

Figure S1…….. p 22

Figure S2…….. p 23

Figure S3…….. p 24

Supplemental References…….p 25

Supplemental Methods

Participants

Twenty-four unmedicated patients with schizophrenia and 45 healthy control participants completed study procedures. Three unmedicated patients were removed from the final sample after quality control procedures were applied (see below). These data were collected with the primary aim of investigating the hypotheses outlined in the main text and the analyses presented here have never been reported previously, although a subset of the healthy control sample was used to characterize the neural correlates of self-ordered working memory task (SOT) performance in a prior report (1) and simple activation data in DLPFC was associated with positron emission tomography measures of cortical DA release in 16 patients and 18 controls in a separate report (2). We also included a sample of 30 demographically matched medicated patients who completed our experimental procedures during the baseline assessment of a randomized controlled trial; 20 of these patients will be included in a forthcoming report along with post-treatment data (3) not relevant to the hypotheses and aims of the present report. None of these reports include the primary analyses reported here, nor do they have any bearing on the hypotheses investigated here.

Task Procedures

Self-ordered Working Memory Task

The SOT consisted of 24 trials, with eight steps of gradually increasing working memory (WM) load in each trial. At the start of a trial, a three-by-three grid of eight simple line drawings of three-dimensional objects was presented, with the center position in the grid left blank. Stimuli were identical to those employed in prior work (1,4,5). Unique stimuli were used on each of the first 12 trials (96 total stimuli) and were each repeated once in the following 12 trials. Participants were given seven seconds in which to respond on each step. Responses consisted of using an fMRI compatible trackball to position a cursor over one of the objects and select it with a button press. Participants were instructed to select any object on each step that they had not already selected on a previous step (thus, on the first step all possible responses are correct). Once participants made a selection, a white square was displayed around the selected object until a total of nine seconds had elapsed since the beginning of the step, thus ensuring that each step remained the same length regardless of participants' reaction times. At the start of each subsequent step after the first, the objects were pseudo-randomly rearranged in the grid, but with the blank space placed at the location of the previously selected item (thus

preventing participants from simply selecting the same location on each step). If participants failed to make a response within seven seconds from the beginning of a step, a white square was displayed around a randomly selected object that would have been a correct response. Participants were instructed to remember this object as if they had selected it themselves, and to continue the trial. If an incorrect selection was made, a red square was displayed over top of the selected object in order to indicate that an error had been made, and the same procedure as in the case of no response was followed. Finally, participants also carried out three trials of a control task, in which one of the objects on each step was marked with an asterisk and participants were instructed to simply select the marked object. In all other respects the display and randomization of stimuli for the control task was identical to the SOT. Unique stimuli were used for each of the control trials, and each trial of either type was preceded by textual instructions indicating whether the upcoming trial was a task trial or a control trial.

Maximum-likelihood Estimation of WM Capacity

Performance data from the SOT was used to obtain an estimate of WM capacity using a simplistic model of WM that assumes that participants carry out the task by loading items into WM until their capacity is reached, and guessing randomly among items not maintained in WM at supra-capacity WM loads. This model is heavily based on maximum-likelihood models commonly used to estimate WM capacity from change detection tasks (6), and was developed in prior work (5). Briefly, the model first assumes that a participant making a response at step *S* of an SOT task with a display of *N* items (in this case, 8 items) will have *m* items maintained in WM, such that

$$m = \min(S - 1, k),$$

where *k* is the participant's WM capacity. The probability, *E*, of the participant making an error can then be shown (under the assumptions outlined above) to be

$$E = \frac{s-1-m}{N-m}.$$

Next, it is assumed that participants will occasionally make errors for reasons other than limited WM capacity, for example due to a lapse in attention or motor response. Thus, an attention parameter is introduced to adjust the formula for *E* such that

$$E = a\frac{s-1-m}{N-m} + (1 - a).$$

Finally, the two free parameters *a* and *k* can be estimated by using a brute-force search of the model space and selecting the value of each parameter that is maximally likely to have produced the observed performance data. For a more complete explanation and justification of the model, see (5).

fMRI Procedures

fMRI Acquisition

The fMRI data acquisition methodology was identical to that reported in Study 2 of our previous report (1). Data was acquired with a Philips 1.5 T Intera scanner equipped with an 8-channel sensitivity-encoding (SENSE) coil at the Columbia Radiology MRI Center at the Neurological Institute of New York. Participants viewed stimuli via a mirror mounted on the head coil, which reflected images projected onto a screen at the foot of the scanner bed. T1-weighted structural scans were acquired with an SPGR sequence using 256 mm FOV, 200 slices, and 1 mm isotropic voxels. Functional echo-planar imaging (EPI) scans were obtained with a SENSE factor of 1.5, 2 s TR, 28 ms TE, 77° flip angle, 192 mm field of view, 40 slices, and 3 mm isotropic voxels. EPI scans covered the entire brain excepting the ventral most portion of the cerebellum. The SOT was spread across 9 functional runs of 160 volumes, each of which included either three task trials or two task trials and one control trial positioned between the two task trials. Each trial was followed by thirty seconds of rest, and the first trial in each run was preceded by 32 seconds of rest.

fMRI Preprocessing

Preprocessing was carried out with SPM8 and custom MATLAB scripts. Data were first slice-timing corrected in SPM8 and then motion realigned with INRIAlign (7). Runs in which participants exhibited greater than 2.5 mm translation or 2.5° rotation from their median position were excluded. Each volume in each run was then evaluated for artifacts, such that any volume whose average in-brain voxel value, or Mahalanobis distance, departed from a sliding window by more than eight mean absolute deviations, was flagged as bad. Flagged volumes were then modeled out during first-level modeling via inclusion of a dummy regressor.

T1 and EPI images were manually aligned to the appropriate International Consortium for Brain Mapping (ICBM) template to provide better initial positioning for coregistration. Functional runs were coregistered to each other and to T1 images, and these were all coregistered to the ICBM template. T1 images were segmented and spatial normalization parameters from the segmentation algorithm were used to warp T1 and EPI images into ICBM standard space. Functional volumes were smoothed with an 8 mm full width at half-maximum (FWHM) Gaussian kernel. Finally, each voxel value in the full timeseries was divided by the mean value in that voxel throughout the run and multiplied by 100. This procedure scales the

magnitude of the hemodynamic response function (HRF) estimates to percent signal change units and ensures that they are equivalently scaled across runs.

First-level Modeling

Preprocessed data was modeled in the SPM8 GLM framework using a three-parameter HRF model, which includes temporal and dispersion derivatives of the canonical HRF. The justification for employing this model rather than a standard one-parameter model is provided elsewhere (1). Automatic masking by SPM8 was disabled and an explicit mask was created from the conjunction of a smoothed gray matter segmentation (6 mm FWHM) and the mean EPI image for each subject, which effectively restricts analyses to gray matter and regions not suffering from excessive signal dropout due to susceptibility artifacts, respectively. Each step of the SOT and the control task was modeled with separate regressors as a nine second boxcar (resulting in 27 regressors in total, due to the three parameter HRF model). Error trials on any of the task steps and on the control task made up two additional sets of regressors, again modeled as a nine second boxcar. A two second boxcar was used to model instruction presentation before each trial, and button presses and error feedback were modeled as instantaneous events whenever they occurred. In addition, several nuisance regressors were included, which were not convolved with the HRF. These were the six motion parameters, the square of these motion parameters, their first derivative, their squared derivative, and dummy indicators for artifactual volumes as described above.

Second-level Modeling

Activation at each step of the SOT and during the control task was quantified as the area under the curve (AUC) in a temporal window ranging from 2 s to 9 s with respect to the three basic functions defining the canonical HRF. This AUC measure is more informative about the magnitude of activation than a standard beta estimate because we employed a three-parameter HRF model in which the estimated parameters (betas) cannot be interpreted as scaling factors of the HRF because they enter the HRF formula nonlinearly. The three-parameter HRF varies in width, timing and height, and the AUC measure employed here captures the information in these additional dimensions.

Corrections for Multiple Comparisons

All second-level analyses of fMRI data presented here were corrected for multiple comparisons using AlphaSim (a MATLAB implementation of the AFNI algorithm included in NeuroElf; www.neuroelf.net) with an activation threshold of $P < .05$, and with smoothness estimated empirically from the model residual maps for each subject. The number of voxels required for a

cluster to achieve significance was thus calculated separately for each analysis, as the correct value depends both on the estimated residual smoothness and on the search volume (e.g., ROI vs. whole-brain). While low *P* value thresholds such as that used here have been criticized for their lack of neuroanatomical specificity (8), these concerns are not especially relevant to the present report because at no point do the primary hypotheses tested here depend on activation having occurred at a given voxel (or set of voxels) rather than some other voxel within the same AlphaSim-identified cluster.

Region of Interest

The ROI was determined by taking the intersection of an anatomical mask obtained from the WFU PickAtlas Brodmann areas 9 and 46 and regions showing significant WM activation in a meta-analysis of healthy individuals (9), dilating the result by 1 voxel, and further masking the result with the set of voxels determined to be gray matter (via SPM segmentation) in every subject included in the study. Exploratory whole-brain analyses were also carried out for the contrast of Task-Control activation. Exploratory analyses for the inverted-U fit were restricted to voxels showing a significant positive fit to the inverted-U in at least one of the three groups, to exclude regions not demonstrating an inverted-U response in at least one group.

Multiple Regression Modeling

As described in the main text, a step-forward model selection was used in a multiple regression framework including diagnostic and medication status indicator variables, symptom measures (the three PANSS subscales), and fMRI outcome measures from four brain regions (inverted-U beta fit from two regions of left lateral prefrontal cortex, and task activation levels in bilateral medial prefrontal cortex and cuneus). Model selection began by evaluating all possible models including the diagnostic indicator variable and one additional variable (among those listed above). The variable with the smallest *P* value was selected and retained, and again all possible models including the diagnostic indicator and the previously selected variable were evaluated. This procedure continued until none of the evaluated models added a variable with $P < .1$. If at any time a variable added in a prior step had a *P* value $> .1$ it would have been removed, although this did not occur. This resulted in a model including (in the order in which they were added) medial PFC activation, precuneus activation, inverted-U fit in the smaller left DLPFC region, and medication status, in addition to the diagnostic status indicator variable included in all models. At this stage, all possible models with a single second-order (interaction) term were evaluated under the same criteria described above. This resulted in the inclusion of a term for the interaction of medial PFC activation and diagnosis, but no other second-order terms. Third-

order terms including this interaction were also evaluated, but none were included. Inclusion of the interaction term caused the main effect of medial PFC activation to become non-significant (P = .30), but the main effect term was retained in the model because the interaction term is uninterpretable without it. Prior to modeling, activation and inverted-U fit measures were transformed to a standard normal deviate (mean subtraction and division by standard deviation), which resulted in the following beta parameters (which can be interpreted as the change in WM capacity with a 1-standard deviation increase in the imaging measure, or when going from controls to patients or from unmedicated patients to medicated patients, as appropriate): diagnostic status, B = -1.07, P = .0074; medication status, B = -.74, P = .053; precuneus activation, B = .84, P < .00001; left prefrontal cortex inverted-U fit, B = .40, P = .006; medial PFC activation, B = -.24, P = .300; medial PFC activation interaction with diagnostic status, B = -1.08, P = .0009.

Table S1. Regions showing significant differences in activation between the SOT and a control task in healthy controls

Region	BA	Cluster Center			Voxels	Max *t*
		x	y	z		
Regions showing greater activation in the SOT than in the control task						
Bilateral Inferotemporal Cortex / Fusiform Gyrus	37	-42	-60	-14	489	8.4748
	19, 37	45	-63	-11	416	7.8747
	37, 20	-36	-42	-17	218	3.9054
	19	-24	-66	-14	82	3.2551
	19, 20	33	-45	-17	140	3.2478
Bilateral Intraparietal Parietal Sulcus / Posterior Parietal Cortex	7	-27	-63	43	581	8.1195
	39	30	-63	43	528	7.7147
	40	42	-39	49	161	4.3171
	40	-42	-39	43	158	4.2796
Bilateral Occipital Lobe	19, 18	-33	-84	13	351	7.0128
	19, 18	36	-81	13	404	5.1529
	18, 17	-21	-90	1	91	3.5938
Medial Parietal Cortex	7	6	-66	52	520	6.7218
Midbrain	-	3	-27	-17	86	3.9458
Bilateral Dorsolateral Prefrontal Cortex	46, 9	-45	24	25	526	10.0605
	46	-39	33	10	139	3.2199
	9, 46	48	21	28	86	4.6437
	46, 9	42	39	25	95	3.8814
	46	42	36	19	68	3.5234
Bilateral Pre-supplementary Motor Area	6, 8, 32	-3	18	46	399	6.8998
Bilateral Premotor Cortex	6	-33	3	52	284	4.7722
	6	-51	-3	40	131	3.7201
	6, 9	48	9	28	118	4.571
	6	27	3	58	88	4.757
	6	30	6	49	76	4.6376
	6, 8	30	15	55	44	4.3227
Regions showing greater activation in the control task than in the SOT						
Bilateral Temporoparietal Cortex	39	-48	-63	22	442	-8.5424
	40	-57	-45	28	162	-7.2119
	22, 39, 40	-60	-54	16	55	-4.6545
	22, 39	-57	-54	7	110	-4.3477
	42, 40	-60	-30	19	88	-3.606
	39	54	-54	22	666	-7.3152
Bilateral Superior and Middle Temporal Gyrus	21, 22	-60	-18	-14	148	-6.6067
	21, 20	-51	-9	-26	55	-5.3647
	21, 20	-42	-3	-32	40	-3.9444
	22, 21	-63	-42	1	52	-3.8553

Region	BA	Cluster Center			Voxels	Max *t*
		x	y	z		
	21, 22	-54	-27	-8	95	-3.4391
	22	-57	0	1	48	-2.7633
Bilateral Temporal Pole	21, 38	-54	0	-23	127	-6.0932
	38, 21	-42	9	-32	52	-5.5016
	22	-60	-39	16	139	-5.2096
	38, 21	-48	12	-26	46	-5.1984
	21	48	3	-26	183	-5.2131
	21	57	-18	-8	447	-5.4363
Bilateral Inferior Frontal Gyrus / Insula	47, 13	-33	15	-17	112	-4.9593
	47, 45	-48	30	-8	44	-2.9065
	47, 45	45	30	-5	281	-5.6666
Bilateral Medial Prefrontal Cortex	10, 32	3	54	4	1217	-9.9032
Bilateral Subgenual Cingulate Cortex	32	-3	33	-11	418	-5.3865
Bilateral Anterior Prefrontal Cortex	9	-15	45	34	547	-6.6294
	8, 9	12	42	43	431	-6.1482
Bilateral Insula	13	36	-3	4	184	-4.4785
	13	57	-30	16	484	-4.1393
	13	-39	-21	10	132	-3.6335
	13	-36	3	4	103	-4.2801
Right Striatum	-	18	12	-14	233	-3.3256
Left Cuneus / Posterior Cingulate	18, 30	-9	-60	1	313	-6.5183
	18, 17	-6	-78	-2	87	-3.1398
Bilateral Precuneus		0	-63	28	700	-5.7625
Bilateral Dorsal Cingulate	24, 31	0	-21	43	460	-5.5837
		0	6	31	51	-3.7745

Cluster center determined as the minimum weighted geometric distance from all voxels in a cluster, with weights determined by voxel *t* values. Clusters of 200 or more voxels were subjected to subclustering by a higher-values-first watershed searching algorithm, with a minimum distance of 8 mm between clusters, and identified subclusters were subsequently reported as separate peaks. Cluster coordinates are given in International Consortium for Brain Mapping (MNI) space.

BA, Brodmann area; SOT, self-ordered working memory task.

Table S2. Regions showing significant differences in activation between the SOT and a control task in unmedicated patients

		Cluster Center				
Region	**BA**	**x**	**y**	**z**	**Voxels**	**Max *t***
Regions showing greater activation in the SOT than in the control task						
Bilateral Fusiform Gyrus / Lateral Occipitotemporal Cortex	37, 19	-39	-63	-11	485	10.5711
	37	33	-42	-17	255	6.9572
	37, 20	-30	-42	-23	246	6.5629
	19, 37	42	-63	-11	426	5.9657
Bilateral Occipital Cortex	18, 19	30	-84	7	393	9.1948
	18, 19	-24	-87	1	300	7.0036
	19	-30	-81	22	288	4.4758
	18	-3	-90	16	47	3.0807
Bilateral Intraparietal Sulcus / Posterior Parietal Cortex	7	-27	-60	46	403	7.6512
	40	45	-36	46	228	3.7787
	40	-45	-24	43	165	3.7005
	7	27	-51	55	95	3.4677
Bilateral Dorsolateral Prefrontal Cortex	46, 9	-45	27	22	422	7.5895
	46	42	33	22	257	10.1613
	9, 6	45	12	28	129	5.9181
	9, 8	48	27	34	57	4.8478
	46, 9	39	42	25	48	3.5523
Bilateral Premotor Cortex	6	-36	0	49	313	6.1501
	6	30	3	55	393	6.3388
Right Temporoparietal Cortex	19, 7	27	-69	40	495	5.9835
Bilateral Frontal Pole	10	-33	51	7	159	5.2219
	10	30	57	7	92	5.8855
Cerebellum	-	0	-63	-17	89	4.0434
Bilateral Medial Parietal Cortex	7	-3	-72	46	88	2.6405
Bilateral Anterior Insula / Striatum	13, -	-21	18	-5	178	4.8832
	13	36	24	1	66	3.9116
	-	21	9	-5	92	4.4108
Thalamus	-	0	-21	10	84	3.2316
Bilateral Pre-Supplementary Motor Area	6, 8, 32	0	21	43	253	4.7993
Regions showing greater activation in the control task than in the SOT						
Right Anterior Middle Temporal Gyrus	21	51	-12	-23	101	-7.222
Bilateral Medial Prefrontal Cortex	11	0	54	-14	89	-5.1582
	11, 10	6	45	-11	46	-4.755
	10	-9	54	19	94	-3.8213
	10	-9	57	10	50	-3.7296
	9	6	48	22	44	-3.2954
	10	-3	57	-2	55	-3.1932

Region	BA	Cluster Center			Voxels	Max *t*
		x	y	z		
Bilateral Precuneus / Posterior Cingulate	31, 23	-6	-48	31	79	-4.9964
	23, 31	-3	-54	22	102	-3.832
Bilateral Medial Posterior Cingulate	31	3	-24	49	62	-4.5678
	31	-12	-33	43	51	-4.481
	31	9	-27	46	56	-4.1109
Right Supplementary Motor Area	6	9	-9	58	44	-4.0389
Bilateral Angular and Supramarginal Gyrus	40	-57	-39	34	115	-7.1387
	39	-51	-60	37	83	-3.4267
	40, 39	57	-57	34	82	-3.8651

Cluster center determined as the minimum weighted geometric distance from all voxels in a cluster, with weights determined by voxel *t* values. Clusters of 200 or more voxels were subjected to subclustering by a higher-values-first watershed searching algorithm, with a minimum distance of 8 mm between clusters, and identified subclusters were subsequently reported as separate peaks. Cluster coordinates are given in International Consortium for Brain Mapping (MNI) space.

BA, Brodmann area; SOT, self-ordered working memory task.

Table S3. Regions showing significant differences in activation between the SOT and a control task in medicated patients

		Cluster Center				
Region	**BA**	**x**	**y**	**z**	**Voxels**	**Max *t***
Regions showing greater activation in the SOT than in the control task						
Bilateral Fusiform Gyrus / Inferotemporal Cortex	37, 19	-42	-60	-14	458	7.5982
	19, 37	-33	-45	-14	103	3.021
	37	33	-42	-17	70	3.0931
Bilateral Occipital Cortex	18, 19	-27	-84	-2	553	7.419
	18, 19	-21	-87	19	157	3.817
	18, 19	33	-72	-8	576	7.5101
	19	30	-75	31	330	7.4692
Bilateral Intraparietal Sulcus / Posterior Parietal Cortex	40, 7	36	-51	49	281	3.65
	7	-18	-69	40	65	6.2522
	7	-21	-60	46	101	5.3297
	40, 39, 7	-36	-54	43	188	4.4107
	7	-24	-72	46	121	4.3632
Bilateral Premotor Cortex	6	-48	0	34	109	6.7003
	6	-45	3	46	86	6.2985
	6	-30	6	52	51	3.6001
	6	42	6	34	72	3.4882
Bilateral Dorsolateral Prefrontal Cortex	9	-45	12	31	123	5.8164
	9, 46	-51	24	22	70	5.4085
	46	-42	33	16	86	3.9664
	9, 46	-45	30	31	46	3.1144
	46, 9	45	30	25	178	7.7915
	9	42	36	34	51	4.5154
Left Anterior Prefrontal Cortex	10, 46	-36	51	13	69	4.2934
Bilateral Pre-Supplementary Motor Area	8, 6, 32	-3	21	46	145	4.5437
Regions showing greater activation in the control task than in the SOT						
Bilateral Temporal Pole	21, 20	-51	-3	-26	89	-3.9539
	21	48	9	-29	56	-4.259
	21, 20	48	-3	-29	43	-3.4281
Right Middle Temporal Gyrus	21, 22	63	-21	-8	121	-5.1319
Right Ventrolateral Prefrontal Cortex / Insula	47, 13	33	24	-17	128	-3.83
	45, 47	48	36	-2	48	-3.3419
Bilateral Subgenual Cingulate	32, 24	-3	36	-8	452	-6.1474
Bilateral Anterior Prefrontal Cortex	9	9	51	22	367	-5.555
	10	-15	54	22	119	-3.3189
Left Globus Pallidus / Thalamus	-	-12	-3	-14	189	-4.3801
Right Anterior / Ventral Striatum	-	18	12	-5	87	-4.2551
Bilateral Medial Prefrontal Cortex	10, 11	3	57	-5	213	-3.8633
Left Temporoparietal Cortex	39	-51	-60	22	128	-3.4772

Cluster center determined as the minimum weighted geometric distance from all voxels in a cluster, with weights determined by voxel *t* values. Clusters of 200 or more voxels were subjected to subclustering by a higher-values-first watershed searching algorithm, with a minimum distance of 8 mm between clusters, and identified subclusters were subsequently reported as separate peaks. Cluster coordinates are given in International Consortium for Brain Mapping (MNI) space.

BA, Brodmann area; SOT, self-ordered working memory task.

Table S4. Regions showing significant positive fit to an inverted-U pattern of activation in healthy controls

		Cluster Center				
Region	**BA**	**x**	**y**	**z**	**Voxels**	**Max *t***
Bilateral Occipital Cortex	19	33	-75	22	521	8.2434
	19	-33	-81	22	271	5.6942
	19, 18	-42	-81	-5	88	3.5443
Bilateral Inferotemporal Cortex / Fusiform Gyrus	37	-36	-51	-17	789	7.7762
	37	39	-45	-17	559	6.4654
	37, 19	42	-66	-5	282	3.9052
Bilateral Intraparietal Sulcus / Posterior Parietal Cortex	7	21	-63	52	426	6.5356
	40, 7	-36	-51	43	265	4.6368
	40	45	-36	52	150	3.6036
Left Medial Parietal Cortex	7	-15	-69	49	372	6.4
Bilateral Medial Temporal Lobe / Hippocampus / Parahippocampal Gyrus	-	30	-9	-26	172	5.1236
	-	-21	-33	-5	102	3.4256
Left Middle Temporal Gyrus	22, 21	-54	-42	-8	323	4.6408
Bilateral Putamen	-	27	0	-5	159	4.2749
	-	-27	0	-2	72	6.3296
	-	-24	9	1	80	5.1099
	-	-27	-6	-14	48	3.0056
Right Posterior Thalamus	-	18	-27	-11	67	3.13
Bilateral Cerebellum	-	6	-48	-23	47	2.8318
Left Insula	13	-33	-9	10	46	4.7503
Bilateral Dorsolateral Prefrontal Cortex	9, 6	-48	12	25	691	9.062
	46	-42	39	7	390	7.5752
	9	39	36	28	106	4.8424
	46	42	39	13	78	4.5837
	46	48	36	19	47	4.279
Bilateral Premotor Cortex	6	-27	6	55	433	7.5416
	6, 9	57	9	25	53	4.1195
	6	27	-3	55	130	6.4111
	6	27	12	55	98	5.0441
Bilateral Pre-Supplementary Motor Area	6, 8, 32	-6	18	46	152	5.2928
	6, 32	6	3	55	54	2.5964
Left Ventrolateral Prefrontal Cortex	44, 45	-54	18	1	78	2.9275

Cluster center determined as the minimum weighted geometric distance from all voxels in a cluster, with weights determined by voxel *t* values. Clusters of 200 or more voxels were subjected to subclustering by a higher-values-first watershed searching algorithm, with a minimum distance of 8 mm between clusters, and identified subclusters were subsequently reported as separate peaks. Cluster coordinates are given in International Consortium for Brain Mapping (MNI) space.

BA, Brodmann area.

Table S5. Regions showing significant positive fit to an inverted-U pattern of activation in unmedicated patients

		Cluster Center				
Region	**BA**	**x**	**y**	**z**	**Voxels**	**Max *t***
Bilateral Fusiform Gyrus	37	33	-51	-14	107	4.0926
	37	-36	-51	-14	120	4.166
Bilateral Dorsolateral Prefrontal Cortex	9, 46	-45	24	28	149	3.8526
	9, 46	39	39	28	81	3.9992
Bilateral Posterior Parietal / Occipitotemporal Cortex	7	18	-69	52	104	4.7802
	7, 19	30	-63	49	55	3.5673
	7, 19	-24	-69	40	181	7.3087
	40	-36	-42	40	43	4.6142
	19, 39	-30	-78	28	57	3.2016
	40	39	-42	52	78	3.6381
Right Occipital Cortex	19	30	-78	31	80	4.601
Left Medial Parietal Cortex	7	-9	-63	52	49	3.4692
Bilateral Premotor Cortex	6	27	9	55	88	4.9204
	6	-30	6	58	149	4.2058
Left Pre-Supplementary Motor Area	6, 32	-3	9	55	62	4.117
Right Superior Parietal	5, 4	9	-39	70	66	4.6848

Cluster center determined as the minimum weighted geometric distance from all voxels in a cluster, with weights determined by voxel *t* values. Clusters of 200 or more voxels were subjected to subclustering by a higher-values-first watershed searching algorithm, with a minimum distance of 8 mm between clusters, and identified subclusters were subsequently reported as separate peaks. Cluster coordinates are given in International Consortium for Brain Mapping (MNI) space.

BA, Brodmann area.

Table S6. Regions showing significant positive fit to an inverted-U pattern of activation in medicated patients

		Cluster Center				
Region	**BA**	**x**	**y**	**z**	**Voxels**	**Max *t***
Left Middle Temporal Gyrus	22, 21	-57	-48	-5	362	4.9323
Bilateral Posterior Parietal Cortex	7	30	-57	58	108	4.3884
	39, 7	-36	-63	43	368	4.1267
	40	-42	-42	40	95	3.2808
Left Medial Temporal Lobe	- , 30	-21	-42	4	116	4.2703
Left Occipital Cortex	18, 17	-15	-96	7	48	4.1371
	19	-30	-81	25	149	3.0578
Bilateral Posterior Thalamus	-	-15	-24	-8	78	3.6602
	-	12	-33	-2	72	4.4167
Left Motor Cortex	5, 4, 6	-3	-39	64	42	3.0552
	4, 3	-21	-27	61	69	5.0073
Right Occipitotemporal Cortex	19, 39	39	-72	7	292	4.0171
Bilateral Anterior Prefrontal Cortex / Frontal Pole	10, 46	-36	45	7	319	5.4102
	10, 9	-24	51	25	51	2.6333
	10	24	57	7	56	3.4902
Bilateral Dorsolateral Prefrontal Cortex	9, 8	-42	27	34	274	5.3588
	9, 46	39	39	28	141	5.4691
Bilateral Premotor Cortex	6	-39	3	49	298	4.6855
	6	30	0	58	146	4.5178
Bilateral Medial Prefrontal Cortex	11	6	51	-17	97	4.5108
Left Ventrolateral Prefrontal Cortex	45, 44	-51	24	1	152	4.3944
Left Orbitofrontal Cortex	11	-33	39	-14	94	4.2546
Bilateral Pre-Supplementary Motor Area	8, 6, 32	-3	15	46	121	3.4422

Cluster center determined as the minimum weighted geometric distance from all voxels in a cluster, with weights determined by voxel *t* values. Clusters of 200 or more voxels were subjected to subclustering by a higher-values-first watershed searching algorithm, with a minimum distance of 8 mm between clusters, and identified subclusters were subsequently reported as separate peaks. Cluster coordinates are given in International Consortium for Brain Mapping (MNI) space.

BA, Brodmann area.

Table S7. Regions showing group differences in inverted-U fit, or a relationship between inverted-U fit and working memory capacity

		Cluster Center				
Region	**BA**	**x**	**y**	**z**	**Voxels**	**Max *t***
Regions Showing a Better Inverted-U Fit in Controls than in Patients						
Right Amygdala	-	24	-6	-26	42	4.1407
Bilateral Fusiform / Inferotemporal Cortex / Medial Temporal Lobe	-	-33	-24	-23	35	4.0297
	19, 37	-27	-54	-17	120	4.0948
	20, -	36	-36	-20	115	3.7546
Bilateral Putamen	-	-24	-3	-5	70	3.076
	-	27	3	-2	43	2.7186
Left Inferior Frontal Gyrus	46, 45	-45	45	4	62	4.6128
Right Cuneus	18	27	-69	22	62	3.7693
Left Dorsolateral Prefrontal Cortex	9, 6	-48	12	28	155	3.6816
Left Premotor Cortex	6	-18	9	61	116	4.7103
Regions Showing a Better Inverted-U Fit in Medicated than Unmedicated Patients						
Left Amygdala	-	-24	-6	-26	66	5.2188
Left Middle Temporal Gyrus	22	-60	-39	-2	95	3.1034
Left Occipitotemporal Cortex	37, 19	48	-63	1	98	3.4339
Left Cuneus	18	-9	-93	16	36	3.5884
Left Anterior Prefrontal Cortex	9, 10	-27	51	28	99	3.5886
Left Angular Gyrus	39	-48	-63	40	54	3.3876
Bilateral Medial Parietal Cortex	7	0	-57	46	119	4.3901
Regions Showing a Relationship between Inverted-U Fit and WM Capacity in Controls						
Left Inferior Prefrontal Cortex	46, 45, 47	-45	42	-2	84	3.301
Left Dorsolateral Prefrontal Cortex	9	-51	15	28	148	3.1719
Left Posterior Parietal Cortex	7	-21	-63	49	81	2.9121
	40	-42	-42	46	133	4.2347
Regions Showing a Relationship between Inverted-U Fit and WM Capacity in Patients						
Left Dorsolateral Prefrontal Cortex	46	-42	33	16	81	3.2439
	9, 6	-45	9	28	55	3.4153
Regions Showing a Relationship between Inverted-U Fit and WM Capacity in Unmedicated Patients						
Left Inferior Frontal Gyrus	46, 45	-48	33	10	35	3.4185
Left Temporoparietal Cortex	19, 39	-39	-81	19	56	3.5694
Left Premotor Cortex	6	-24	9	58	59	3.6064
Left Fusiform Gyrus	19, 37	-36	-66	-14	40	-3.1745
Left Insula	13	-30	-3	7	69	-3.1302
Regions Showing a Relationship between Inverted-U Fit and WM Capacity in Medicated Patients						
Left Fusiform Gyrus	37	-36	-48	-23	50	3.2771
Bilateral Dorsolateral Prefrontal Cortex	9, 46	39	39	28	74	3.3801
	9, 6	-42	9	31	33	3.0064

Cluster center determined as the minimum weighted geometric distance from all voxels in a cluster, with weights determined by voxel *t* values. Clusters of 200 or more voxels were subjected to subclustering by a higher-values-first watershed searching algorithm, with a minimum distance of 8 mm between clusters, and identified subclusters were

subsequently reported as separate peaks. Cluster coordinates are given in International Consortium for Brain Mapping (MNI) space.

BA, Brodmann area; WM, working memory.

Table S8. Regions showing group differences in activation, or a relationship between activation and working memory capacity

		Cluster Center				
Region	**BA**	**x**	**y**	**z**	**Voxels**	**Max *t***
Regions Showing Differences in Activation Between Patients and Controls						
Bilateral Cuneus	19, 18	-12	-63	-2	300	-4.3912
	18, 19	15	-72	-5	171	-3.9904
	17, 18	-9	-84	7	314	-3.4464
	18	6	-81	22	59	-2.8304
Bilateral Medial Prefrontal Cortex	10, 32	3	51	4	242	-4.1545
	11,10	-6	48	-11	71	-3.5461
	9, 10	0	54	22	86	-3.1764
	10	-6	57	-2	56	-2.9398
Bilateral Dorsal Anterior Cingulate	24, 32	3	27	22	101	-3.6686
Bilateral Middle / Superior Temporal Gyrus	22, 41	54	-12	1	73	-3.1168
	22, 21	-60	-39	7	78	-2.9026
Bilateral Posterior Cingulate	31	6	-42	40	108	-3.7559
Right Motor / Somatosensory Cortex	4, 3, 2	42	-15	43	91	-3.5692
Regions Showing Differences in Activation Between Unmedicated and Medicated Patients						
Bilateral Posterior Parietal Cortex	31	6	-27	49	72	3.9258
Bilateral Putamen / Insula	- , 13	-21	15	-11	183	-3.3482
	13	36	24	-2	189	-3.5852
	-	18	9	-5	164	-4.8298
Left Motor / Somatosensory Cortex	4, 3	-39	-12	52	182	-4.1482
Right Premotor	6	33	0	58	152	-4.4009
Regions Showing a Relationship between Activation and WM Capacity in Controls						
Bilateral Cuneus	18, 17	3	-78	13	140	3.569
Bilateral Medial Dorsal Prefrontal Cortex	9	-3	45	28	62	-3.4177
	9, 10	-9	51	16	58	-3.1192
Right Anterior Prefrontal Cortex	10	21	51	22	95	-3.1229
	9, 10	15	45	31	46	-2.9146
Right Supramarginal Gyrus	40	57	-48	31	76	-3.6287
Left Supplementary Motor Cortex / Cingulate	6, 31	-6	-18	49	78	-3.353
Right Medial Parietal Cortex	7	15	-48	58	81	-3.2859
Regions Showing a Relationship between Activation and WM Capacity in Patients						
Right Putamen	-	18	12	-5	100	4.2068
Bilateral Occipital Cortex	19	-30	-84	19	83	3.1025
	19	33	-78	25	162	3.398
Bilateral Posterior Parietal Cortex	40	39	-45	49	192	3.4934
	7	15	-69	46	399	3.4745
	7	-18	-66	43	257	3.3254

Region	BA	Cluster Center			Voxels	Max *t*
		x	y	z		
	40	-42	-39	46	82	3.1454
Bilateral Pre-supplementary Motor Area	6, 8, 32	6	18	43	116	3.5655
Bilateral Premotor Cortex	6	30	0	58	71	2.657
	6	-30	0	58	79	3.6486
Left Middle / Superior Temporal Gyrus	21, 22	-60	-21	-11	120	-4.7789
	21, 38	-51	3	-26	82	-3.6485
	21, 22	-57	-6	-20	96	-3.5807
Left Ventrolateral Prefrontal Cortex	47	-33	21	-17	53	-3.3406
Bilateral Medial Prefrontal Cortex	10	0	60	-5	109	-3.979
	10	-3	51	10	129	-3.9777
	10, 32	6	51	4	40	-3.3739
	9	-6	48	37	41	-3.1633
Left Anterior Prefrontal Cortex	10	-18	54	28	46	-3.4759
Bilateral Posterior Cingulate / Precuneus	31, 23	0	-54	25	157	-3.2187
Bilateral Supramarginal / Angular Gyrus	39, 40	-51	-54	25	107	-3.472
	39	-45	-66	34	75	-3.2928
	39	-51	-69	25	38	-3.2557
	39	51	-63	31	98	-3.8142
Right Dorsal Prefrontal Cortex	8	12	36	49	78	-3.6691
Regions Showing a Relationship between Activation and WM Capacity in Unmedicated Patients						
Right Inferior Parietal Lobule	40	42	-45	46	85	3.2314
Left Middle Temporal Gyrus	21, 22	-57	-9	-17	190	-3.4073
Bilateral Medial Prefrontal Cortex	10	0	51	7	106	-3.6035
Bilateral Posterior Cingulate / Precuneus	23, 31	0	-57	25	147	-3.4562
Regions Showing a Relationship between Activation and WM Capacity in Medicated Patients						
Left Occipitotemporal Cortex	19, 37	-39	-69	-8	96	3.8918
Right Putamen	-	21	15	-2	143	3.7409
Left Occipital Cortex	19	-30	-78	22	88	2.9129
Bilateral Posterior Parietal Cortex	7	-24	-60	49	81	3.8587
	7	21	-60	55	99	3.8179
	7, 40	33	-54	52	53	2.9436
Bilateral Medial Parietal Cortex	7	12	-69	46	87	3.0955
		-6	-60	55	46	3.0377
	7	-12	-72	46	85	2.9958
Right Occipitoparietal Cortex	19, 7	21	-78	40	40	3.0861
	19, 39	30	-69	34	49	2.892
Right Middle Temporal Gyrus	21, 22	-57	-9	-17	116	-3.8075
Bilateral Medial Prefrontal Cortex	10	0	57	-2	158	-4.4054

Region	BA	Cluster Center			Voxels	Max *t*
		x	y	z		
Left Inferior Motor / Somatosensory / Superior Temporal Cortex	43, 4	-57	-6	13	94	-3.6852
	41, 40	-51	-24	16	98	-3.2756
Bilateral Angular Gyrus	39	51	-63	31	107	-3.5856
	39	-51	-60	28	145	-3.1299
Medial Dorsal Prefrontal Cortex	8	3	36	52	177	-3.5925

Cluster center determined as the minimum weighted geometric distance from all voxels in a cluster, with weights determined by voxel *t* values. Clusters of 200 or more voxels were subjected to subclustering by a higher-values-first watershed searching algorithm, with a minimum distance of 8 mm between clusters, and identified subclusters were subsequently reported as separate peaks. Cluster coordinates are given in International Consortium for Brain Mapping (MNI) space.

BA, Brodmann area; WM, working memory.

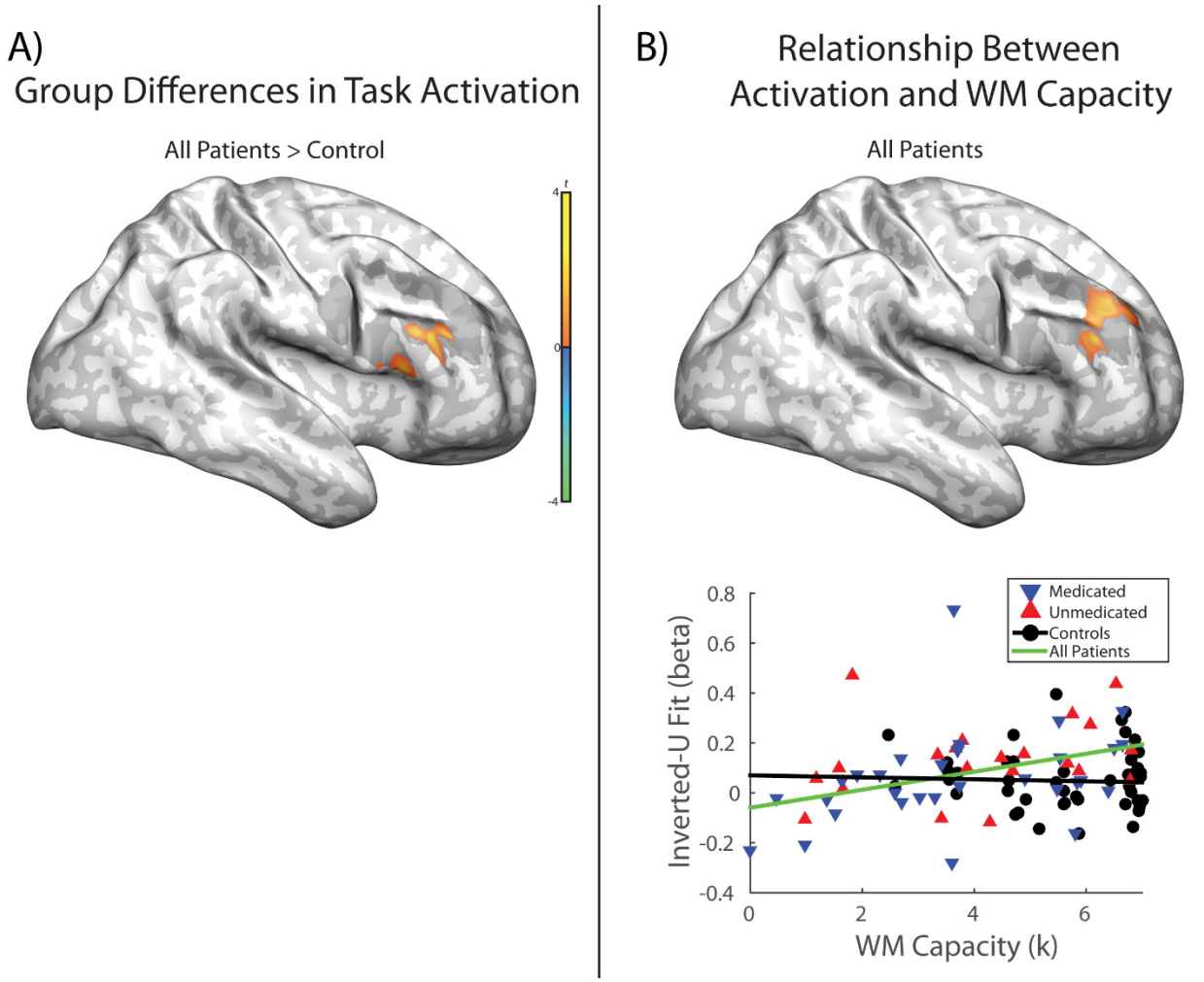

Figure S1. Regions in the dorsolateral prefrontal cortex region of interest showing (**A**) group differences in task activation (61 voxels; MNI coordinates 48, 27, 19; max *t*-value 3.4), and (**B**) a relationship between activation and working memory capacity (60 voxels; MNI coordinates 36, 39, 28; max *t*-value 3.4). The scatter plot shows the average activation within the voxels shown in (**B**) plotted against working memory capacity. Shaded regions show the extent of the region interest of interest.

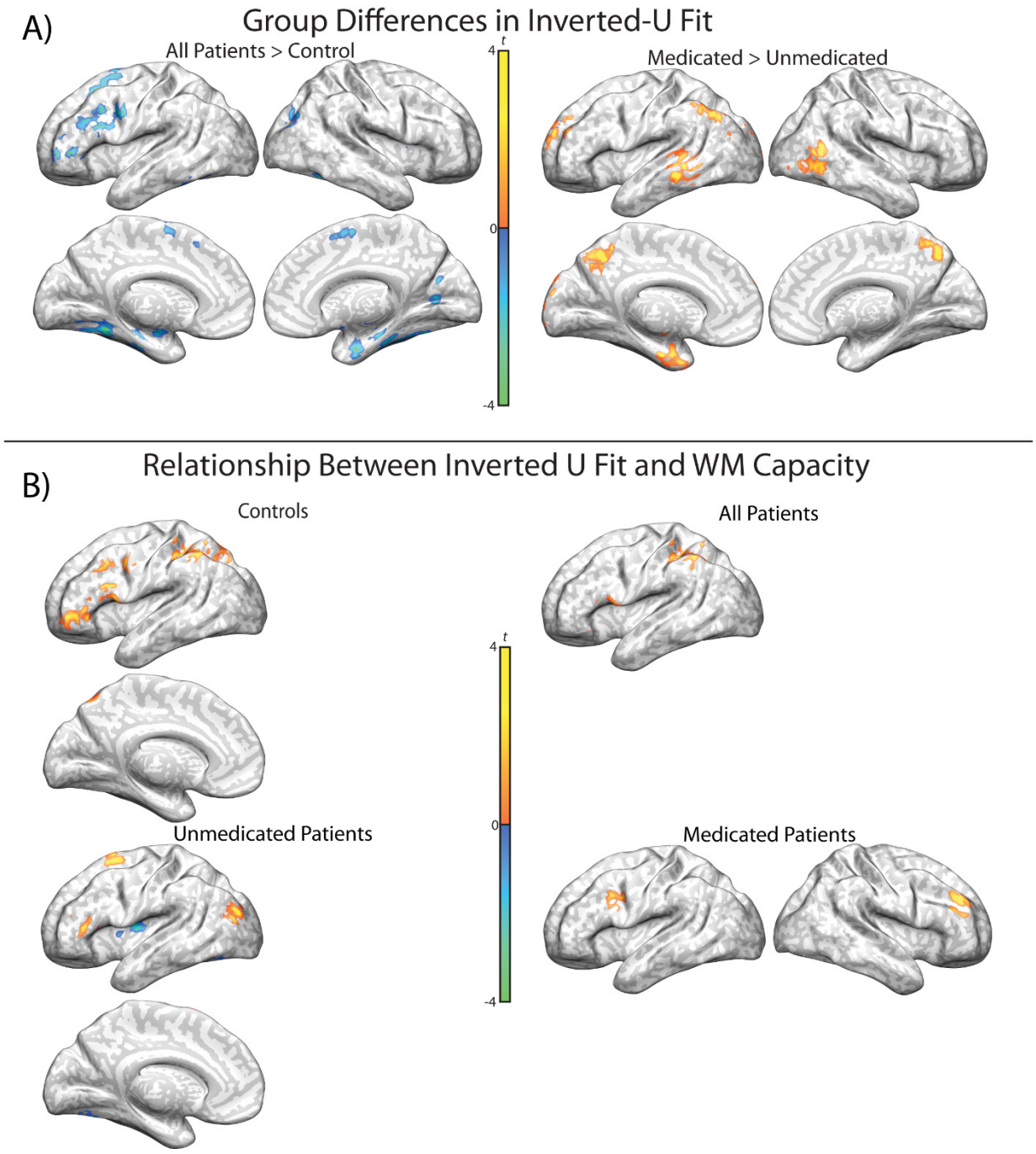

Figure S2. Brain regions showing (**A**) group differences or (**B**) a relationship with working memory capacity in the fit of an inverted-U shape to activation over seven working memory loads.

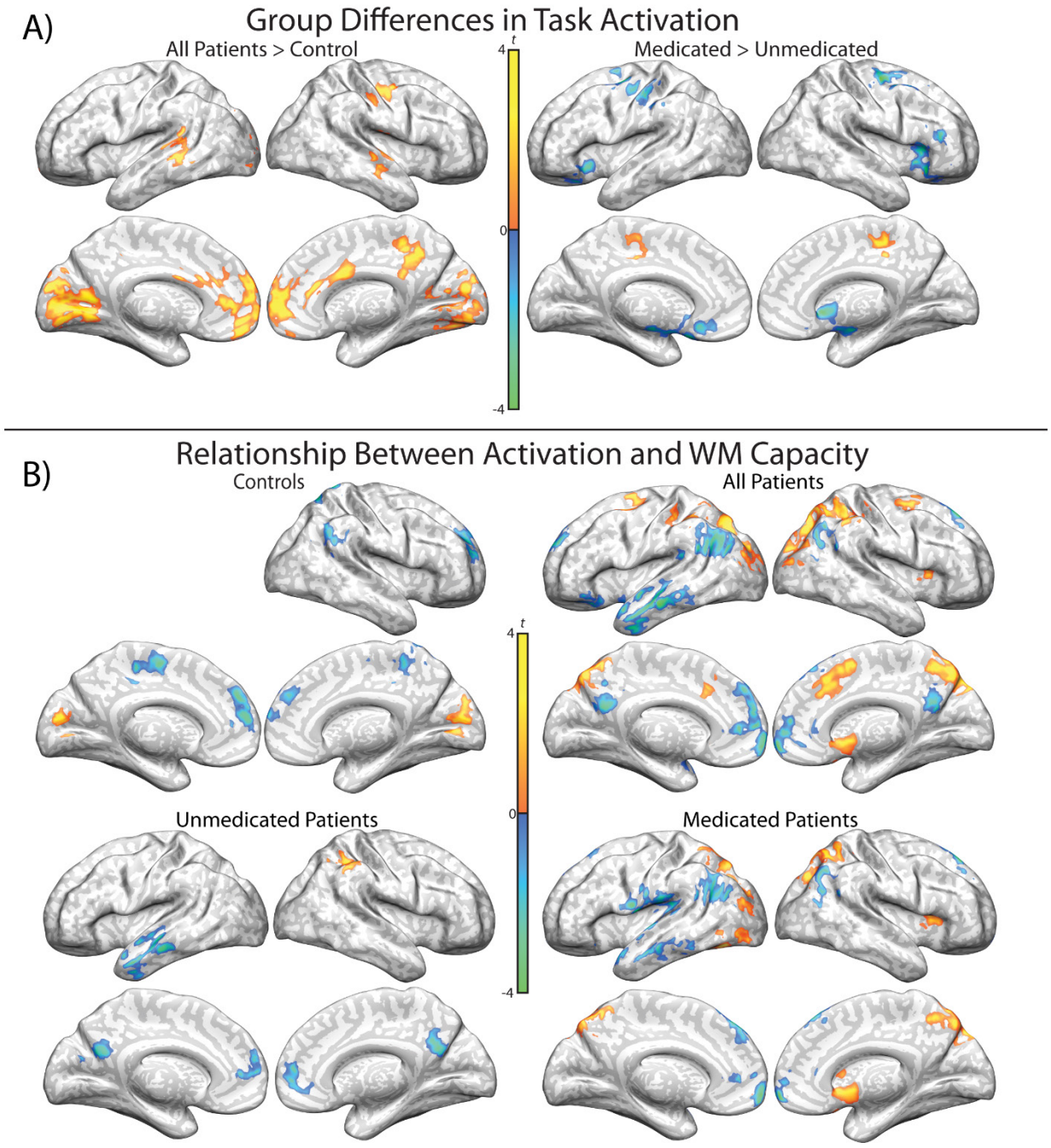

Figure S3. Brain regions showing (**A**) group differences or (**B**) a relationship with working memory capacity in activation to the self-ordered working memory task.

Supplemental References

1. Van Snellenberg JX, Slifstein M, Read C, et al. Dynamic shifts in brain network activation during supracapacity working memory task performance. *Human brain mapping.* 2015;36:1245-1264.
2. Slifstein M, van de Geissen E, Van Snellenberg J, et al. Deficits in prefrontal cortical and extra-striatal dopamine release in schizophrenia: A Positron Emission Tomographic Functional Magnetic Resonance Imaging Study. *JAMA psychiatry.* 2015;72:316-324.
3. Girgis RR, Van Snellenberg JX, Glass A, et al. A proof of concept, randomized controlled trial of DAR-0100A, a dopamine-1 receptor agonist, for cognitive enhancement in schizophrenia. submitted.
4. Curtis CE, Zald DH, Pardo JV. Organization of working memory within the human prefrontal cortex: a PET study of self-ordered object working memory. *Neuropsychologia.* 2000;38(11):1503-1510.
5. Van Snellenberg JX, Conway AR, Spicer J, Read C, Smith EE. Capacity estimates in working memory: Reliability and interrelationships among tasks. *Cognitive, affective & behavioral neuroscience.* Mar 2014;14(1):106-116.
6. Rouder JN, Morey RD, Cowan N, Zwilling CE, Morey CC, Pratte MS. An assessment of fixed-capacity models of visual working memory. *Proceedings of the National Academy of Sciences of the United States of America.* 2008;105:5975-5979.
7. Freire L, Roche A, Mangin J-F. What is the best similarity measure for motion correction in fMRI? *IEEE Transactions in Medical Imaging.* 2002;21:470-484.
8. Woo CW, Krishnan A, Wager TD. Cluster-extent based thresholding in fMRI analyses: pitfalls and recommendations. *NeuroImage.* May 1 2014;91:412-419.
9. Wager TD, Smith EE. Neuroimaging studies of working memory: a meta-analysis. *Cognitive, Affective, and Behavioral Neuroscience.* Dec 2003;3(4):255-274.